Tellus SERIES A DYNAMIC METEOROLOGY AND OCEANOGRAPHY
PUBLISHED BY THE INTERNATIONAL METEOROLOGICAL INSTITUTE IN STOCKHOLM

A striking early-summer event of a convective rainband persistent along the warm Kuroshio in the East China Sea

By TORU MIYAMA[1]*, MASAMI NONAKA[1], HISASHI NAKAMURA[1,2] and AKIRA KUWANO-YOSHIDA[3], [1]*Research Institute for Global Change, Japan Agency for Marine-Earth Science and Technology, Yokohama, Japan*; [2]*Research Center for Advanced Science and Technology, University of Tokyo, Tokyo, Japan*; [3]*Earth Simulator Center, Japan Agency for Marine-Earth Science and Technology, Yokohama, Japan*

(Manuscript received 12 June 2012; in final form 17 October 2012)

ABSTRACT

A narrow, well-defined rainband persisted over the East China Sea on 19–20 May 2010, well separated from the Baiu/Meiyu front to its north. The rainband formed along the Kuroshio, leading us to the hypothesis that its high sea-surface temperature (SST) helped organise and maintain convective precipitation within the warm, moist surface southerlies. This hypothesis is verified through a pair of experiments with a regional atmospheric model. An experiment where high-resolution SST is prescribed as the lower-boundary condition is successful in reproducing the observed rainband. The reproduction is, however, unsuccessful in the other experiment where the narrow band of SST maxima along the Kuroshio has been artificially eliminated by smoothing. These experiments demonstrate that the high SST along the Kuroshio was of critical importance in organising the convective rainband separated from the Baiu/Meiyu front, thus presenting evidence that a mid-latitude western boundary current can influence the overlying atmosphere. Additional experiments suggest that the orography of Taiwan can also contribute positively to the organisation of the rainband by enhancing the convergence of the surface southerlies over the warm Kuroshio.

Keywords: atmosphere-ocean interaction, deep convection, precipitation band, western boundary current, mid-latitude, regional model

1. Introduction

It has been long believed that the mid-latitude ocean varies passively under the strong atmospheric variability. Recent studies, however, have revealed the importance of high sea-surface temperatures (SSTs) along the mid-latitude western boundary currents in organising clouds and precipitation (Xie et al., 2002; Small et al., 2008; Taguchi et al., 2009; Tokinaga et al., 2009). A fundamental question is whether the mid-latitude ocean can influence the free atmosphere beyond the marine boundary layer. While deep convections over high SSTs are common in the tropics, systematic organisation of such deep convections over the mid-latitude ocean has been questionable until very recently. Combining operational atmospheric analyses, satellite observations and an atmospheric general circulation model output, Minobe et al. (2008) have revealed a narrow band of precipitation in the annual climatology organised along the Gulf Stream, accompanied by convective clouds and updraft extending into the upper troposphere. Especially in summer, a deep-heating mode, characterised by latent heating in the mid- and upper troposphere due to deep convection, tends to be observed along the Florida Current and the western Gulf Stream proper (Kuwano-Yoshida et al., 2010; Minobe et al., 2010).

Very recently, regional model experiments and data analyses by Xu et al. (2011) and Sasaki et al. (2012) have demonstrated that deep convective precipitation tends to be organised climatologically also along the warm Kuroshio over the East China Sea, especially in spring and early summer. Likely masked by energetic transient weather systems, the rainband that forms as a response to the warm Kuroshio can be identified

*Corresponding author.
email: tmiyama@jamstec.go.jp

Citation: Tellus A 2012, **64**, 18962, http://dx.doi.org/10.3402/tellusa.v64i0.18962

most unambiguously in a monthly or seasonal-mean field (Xu et al., 2011; Sasaki et al., 2012).

The present study presents a striking event in which the organisation of a narrow convective rainband along the Kuroshio is evident even in a snapshot without taking any time averaging. A radar image in Fig. 1a at 0000 UTC (0900 Japanese Standard Time) on 20 May 2010 indicates a well-organised rainband in the East China Sea to the west of the Okinawa Islands. It extended north-eastward from the immediate north-east of Taiwan (25°N) to the south of the Shikoku Island of Japan (31°N). The rainband shown in Fig. 1a was collocated with a belt of SST maxima along the Kuroshio (Fig. 1b), suggesting that the high SST may be the prime factor for organising the rainband. After emerging around 0600 UTC on 19 May, the particular rainband persisted for more than 20 hours.

Notably, this rainband formed well south of the Baiu/Meiyu front, a quasi-stationary seasonal frontal system as analysed in a weather chart (Fig. 1c). The separation between the rainband and Baiu/Meiyu front is apparent also in a visible cloud image from a geostationary satellite (Fig. 1d), where a band of bright meso-scale spots characteristic of deep convective clouds is distinguishable from a more extensive cloudy area to its north that corresponds to stratiform clouds associated with the Baiu/Meiyu front. Although in a particular event studied by Xu et al. (2011)

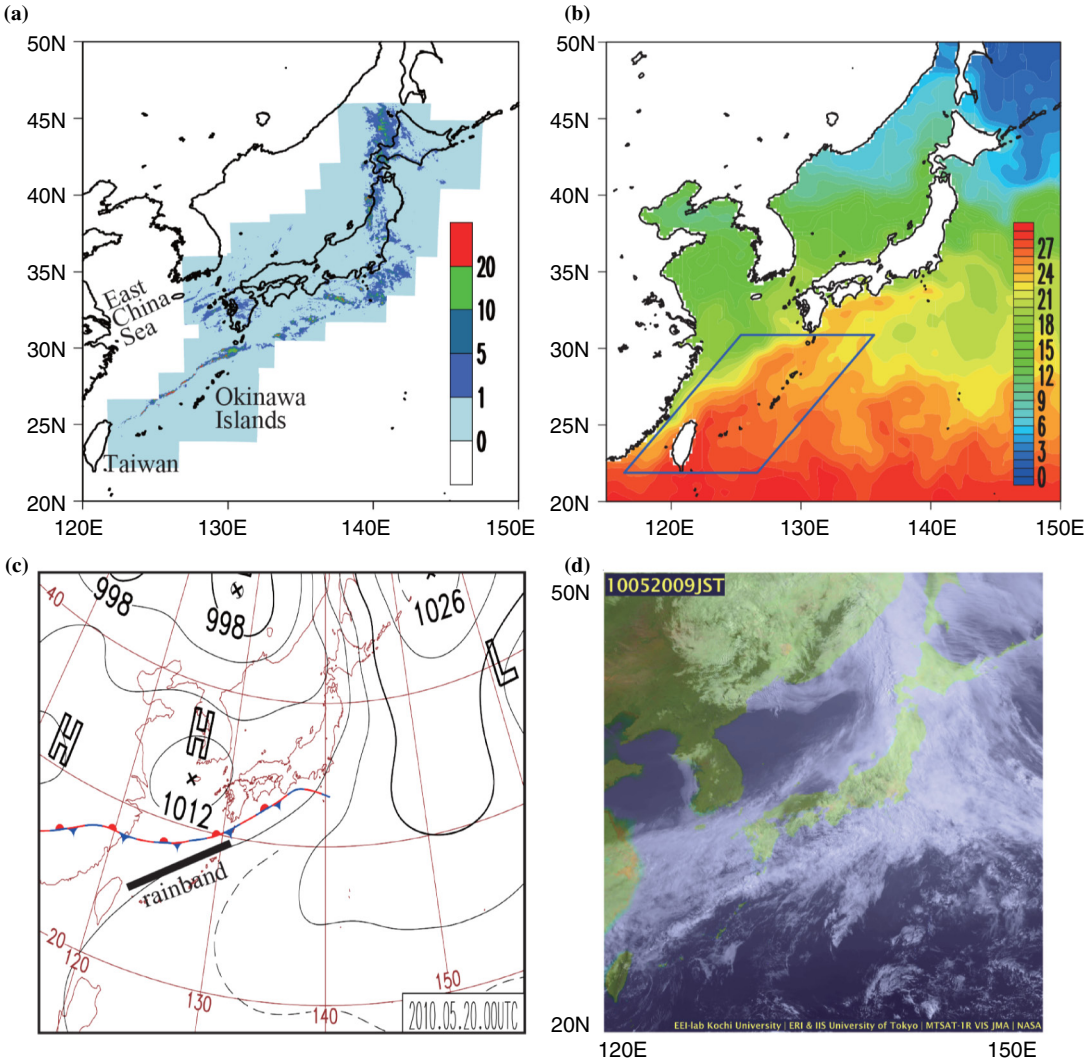

Fig. 1. Observations at 0900 JST (0000 UTC), 20 May 2010. (a) Precipitation (mm h^{-1}) observed with the Japan Meteorological Agency (JMA) radar network. (b) Sea surface temperature (°C; SST) used for the model lower-boundary condition of the CNTL run. In the SMTH run, the same SST field as in (b) is assigned at the model boundary but it has been smoothed. (c) Surface weather map by JMA. The upper part of the original figure is trimmed for better comparison with the other panels. The location of the rainband is added schematically. (d) Visible cloud image by the Geostationary Meteorological Satellite-5 available at the Kochi University (http://weather.is.kochi-u.ac.jp/).

an eastward-moving extratropical cyclone that passed over the Kuroshio is shown to be as an important factor for precipitation enhancement, the rainband event in Fig. 1a should be explained by another mechanism.

On monthly and seasonal time scales, precipitation associated with the Baiu/Meiyu front tends to be organised along the subtropical jet stream whose warm advection induces a large-scale ascent (Sampe and Xie, 2010; Kosaka et al., 2011). In contrast, the rainband in the present study formed well south of a quasi-stationary rain front and the associated subtropical jet aloft, which leads us to a hypothesis that the convective rainband was organised and maintained by high SST along the Kuroshio. We verify our hypothesis by conducting a set of numerical experiments with a regional atmospheric model with and without the SST maxima along the Kuroshio as the model lower-boundary condition.

2. Model and data

A regional atmospheric model based on the hydrostatic primitive equations is used. The model has been developed by Y. Wang of University of Hawaii (Wang et al., 2005) and widely used (e.g. Wang et al., 2003, 2005; Xie et al., 2007; Taguchi et al., 2009). The representation of grid-scale moist processes includes a cloud microphysics scheme developed by Wang (2001). Subgrid-scale convection is parameterised by a mass flux scheme (Tiedtke, 1989; Nordeng, 1994; Gregory et al., 2000).

The model domain set for our experiments is [0–70°N, 90–180°E]. The model resolution is 0.125° in both latitude and longitude, with 28 vertical sigma levels, including 11 levels below the 800-hPa level. The top of the model atmosphere is placed around the 15-hPa level. During time integration, the zonal and meridional wind velocities, air temperature and relative humidity were updated at the lateral boundaries of the domain with 6-hourly fields of the Global Spectral Model (GSM, 0.5° horizontal resolution) analysis provided by the Japan Meteorological Agency (JMA). The initial conditions for our model were taken from the JMA Meso Scale Model (MSM, $0.125° \times 0.1°$ horizontal resolution) analysis for the inner domain of the model [22.4–47.6°N, 120°–150°E], where the MSM data were available, and its outer domain was filled with the JMA GSM data. The GSM/MSM analyses and JMA radar precipitation data for comparison with the model results were obtained from the Research Institute for Sustainable Humanosphere, Kyoto University (http://database.rish.kyoto-u.ac.jp/arch/glob-atmos/). As the model lower-boundary condition, daily-mean fields of high-resolution (0.25° horizontally) SST (Reynolds et al., 2007) were assigned, which are based on measurements with Advanced Very High Resolution Radiometer and Advanced Microwave Scanning Radiometer.

A pair of hindcast experiments are mainly discussed: a control experiment (CNTL) using the original high-resolution SST and the other (SMTH) with the SST field that had been artificially smoothed in space by applying a five-point filter 200 times over the domain surrounded by blue lines in Fig. 1b. For each of the experiments, three-member ensemble integrations were conducted for the 3-day period with three different initial conditions taken from the MSM analysis for 0000, 0300 UTC 18 May, and 2100 UTC 17 May. The ensemble spread among the three members was found small (not shown), and the ensemble mean fields are shown in the following.

3. Results

As shown in Fig. 2b, the CNTL run is overall successful in reproducing the narrow rainband structure in the East China Sea, especially between 24°N and 28°N. As observed (Fig. 2a), the simulated rainband forms along the band of SST maxima along the Kuroshio Current (Fig. 2b), to the south of the stationary front indicated in the weather map (Fig. 1c). As shown in the MSM (Fig. 2d) and also in the CNTL run (Fig. 2e), this stationary front is manifested as sharp gradient in 1000-hPa humidity (from 13 to 16 g/kg), corresponding to the boundary between dry air from the Asian continent and humid air from the southern ocean, which is characteristic of the Baiu/Meiyu front (Ninomiya, 1984). As actually observed (Fig. 2d), the simulated rainband is collocated with the peak of humidity itself rather than its gradient (Fig. 2e). The humidity distribution in the CNTL run (Fig. 2e) is overall similar to that in the MSM (Fig. 2d), except that the simulated humidity maximum is about $1\ \mathrm{g\ kg^{-1}}$ lower. The strong surface convergence (red hatched in Fig. 2d, e) is also collocated with the SST maxima both in the MSM analysis and in the CNTL run.

A discrepancy in precipitation between the CNTL run (Fig. 2b) and observations (Fig. 2a) is noticeable east of 127.5°E, where the model simulates the rainband to the south of its observed counterpart that coincides with the SST maxima along the Kuroshio axis (Fig. 2a). The rainband observed east of 127.5°E (Fig. 2a) is organised along the Baiu/Meiyu front, marked as a line of surface convergence and tight humidity gradient (Fig. 2d). Unlike in the observations, however, the CNTL run appears to simulate a dual front structure east of 127.5°E: one along the SST peak around 29°N and the other to its south around 28°N (Fig. 2e). In recognition of this discrepancy, we hereafter focus on the south-western portion of the rainband located west of 127.5°E, which forms along the Kuroshio axis well to the south of the Baiu/Meiyu front both in the observations and in the CNTL run.

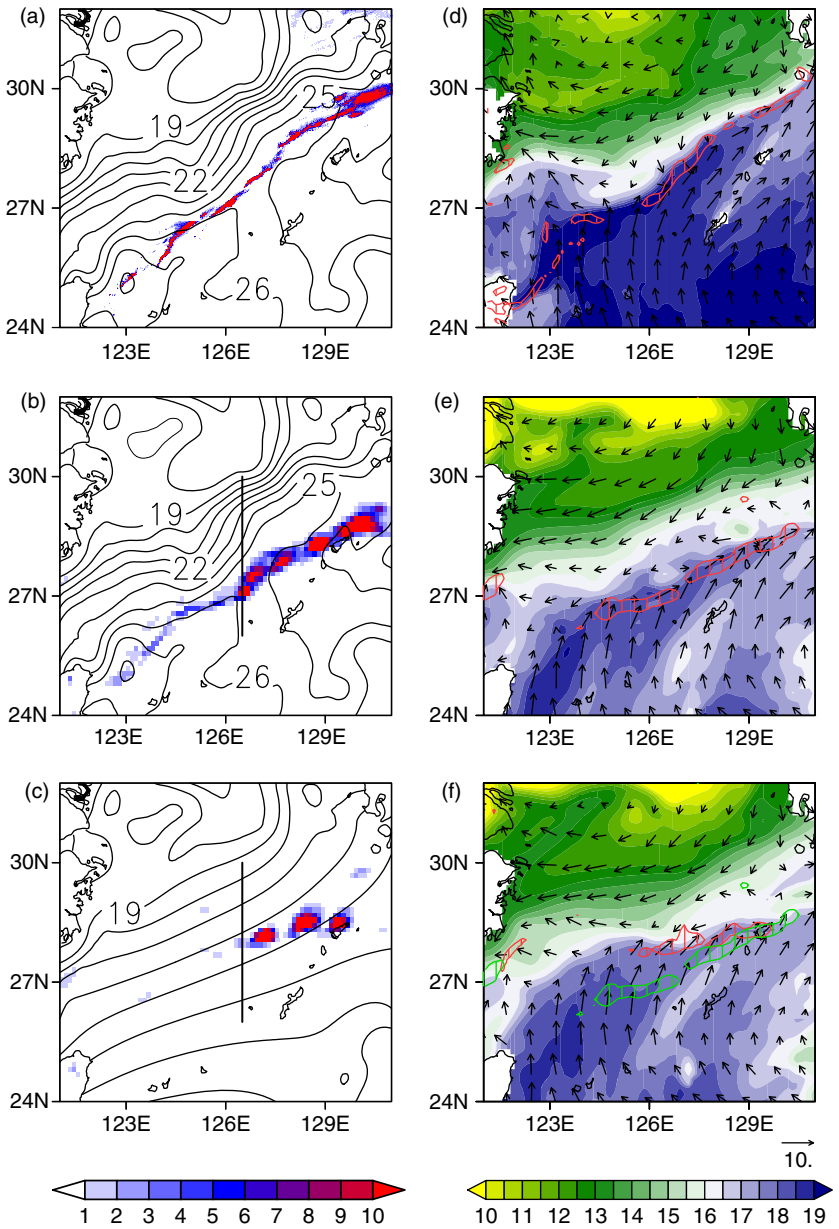

Fig. 2. Comparison of the observation and model results. (Left) SST (°C, contour) and precipitation (mm h^{-1}, shade) based on the (a) radar observation, (b) CNTL run and (c) SMTH run. (Right) 1000-hPa specific humidity (g kg^{-1}, shade) and wind vector (m s^{-1}) based on the (d) JMA MSM, (e) CNTL run and (f) SMTH run. Red hatches in (d)–(f) indicate 1000-hPa wind convergence stronger than 1.0×10^{-4} s^{-1} in the CNTL and SMTH runs, respectively. Green hatch in (f) duplicates the red hatch in (e) for comparison. Meridional lines in (b) and (c) are used for Figs. 3 Fig. 4. All figures at 0900 JST (0000 UTC), 20 May 2010.

The particular rainband cannot be reproduced in the SMTH run (Fig. 2c), where the SST field has been smoothed in space to eliminate the SST maxima along the Kuroshio. The pair of the model runs demonstrates the particular importance of high SST along the Kuroshio in organising the rainband. Most of the reduced precipitation in the SMTH run is accounted for by convective rainfall represented with a subgrid-scale convection parameterisation (as shown specifically in Fig. 5a). Correspondingly, in the SMTH run (Fig. 2f), the moist surface southerlies converge towards the southern flank of the model Baiu/Meiyu front, located farther to the north than in the CNTL run (Fig. 2e). In fact, a band of humidity maxima forms, being confined meridionally to the Kuroshio axis in the CNTL run, whereas the corresponding maxima are much more diffused meridionally in the SMTH run.

The aforementioned differences between the CNTL and SMTH runs can be better illustrated in a meridional section (Fig. 3) for 126.5°E (along the meridional lines in Fig. 2b, c). In the absence of the Kuroshio-associated high SST in the SMTH run (Fig. 3b), a warm humid surface airflow with high equivalent potential temperature θ_e originating from the Tropics converges directly into the model Baiu/Meiyu front around 28°N and then ascends over cold dry air with lower θ_e situated to the north of the surface front (see also Fig. 2f). This ascent at the Baiu/Meiyu front occurs under the subtropical westerly jet (black thick contour lines in Fig. 3b). These features represent typical structure of the Baiu/Meiyu front (Sampe and Xie, 2010). In the CNTL run (Fig. 3a), by contrast, the major ascent is deeper and stronger situated at 27°N, well south of the Baiu/Meiyu front situated below the westerly subtropical jet (Fig. 3b). Anchored by the warm Kuroshio, the ascent at 27°N is associated with deep convection,

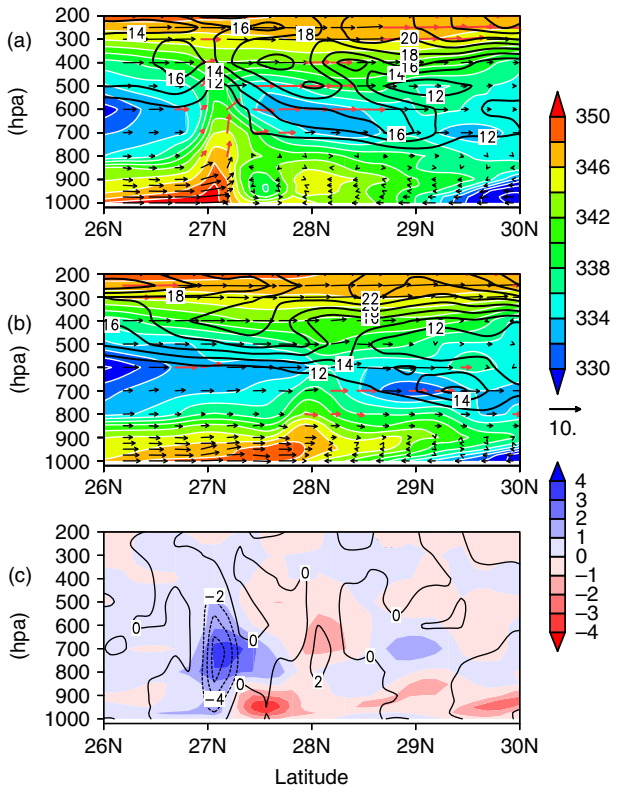

Fig. 3. Meridional vertical sections for 126.5°E (across the meridional lines in Fig. 2b, c) at 0900 JST (0000 UTC), 20 May 2010. (a)–(b) Equivalent potential temperature (K, shade), zonal wind velocity (greater than 12 m/s, thick black contours) and wind vector (m s^{-1} horizontally and Pa s^{-1} vertically), based on the (a) CNTL and (b) SMTH runs. Red arrows highlight wind vectors whose ageostrophic component is northward and greater than 4 m s^{-1}, and otherwise wind vectors are indicated by black arrows. (c) Differences (CNTL minus SMTH) in specific humidity (g kg^{-1}, shaded) and vertical velocity (Pa s^{-1}, contour).

reaching up to the 350-hPa level as the three-member ensemble mean. The individual members simulate the convection that reaches as high as the 200-hPa level. The Coriolis force acting on poleward ageostrophic motion, especially in the mid-troposphere, induced by the convection (red vectors in Fig. 3a) acts to maintain the subtropical jet (thick black contours in Fig. 3a). Since the convection occurs south of the Baiu/Meiyu front, the mid-tropospheric subtropical jet in the CNTL run is displaced slightly southward relative to the SMTH run (the black thick contour in Figs. 3b). The heavy convective rainfall is sustained by moisture transport by the warm, humid southerlies from the Tropics that converge directly into the rainband (Fig. 2e and 3a). The difference (CNTL–SMTH) plot in Fig. 3c suggests that the presence of the Kuroshio can lead to the pronounced enhancement of convective updraft and consequent lower-tropospheric moistening above the Kuroshio axis, while it leads to a slight weakening of the ascent associated with the Baiu/Meiyu front and the consequent drying in the lower troposphere.

Time-latitude sections in Fig. 4 show the evolution of the rainband and its environment simulated in the CNTL run. As evident in Fig. 4a, a humid airmass from the Tropics intrudes northward in the last half of 18 May. Its intrusion below colder and drier air in the mid-troposphere (Fig. 3a) increases the convective available potential energy (CAPE), an indicator of vertical convective instability (shaded in Fig. 4b). In travelling over higher SST (shaded in Fig. 4d) in the CNTL run than in the SMTH run across the Kuroshio axis between 27°N and 29°N, this humid airmass warms up further resulting in a rapid increase in CAPE (contoured and hatched in Fig. 4c) and the subsequent commencement of convective precipitation (contoured in Fig. 4b). In the morning of 19 May (around 0000 UTC), the high-CAPE airmass intrudes most northward (Fig. 4b), and then it retreats back southward for the next 24 hours. In the afternoon of 19 May (0400 ~ 1000 UTC), the boundary between the northerlies and southerlies (thick contour in Fig. 4a) undergoes rapid southward displacement until it reaches the highest CAPE region. At this stage, the high-CAPE region becomes confined meridionally into the northern flank of the SST maxima along the Kuroshio, leading to the local enhancement of precipitation (hatched in Fig. 4b). Compared to the SMTH run, the stronger meridional confinement of the moist air (shaded in Fig. 4c; also shown in Figs. 2 and 3) with higher CAPE (hatched in Fig. 4c) in the CNTL run helps organise the well-defined rainband. Heavy convective precipitation is organised into the narrow zone characterised by both high CAPE (shaded in Fig. 4b) and surface convergence (hatched in Fig. 4a), which moves gradually southward to the SST peak (contoured in Fig. 4d) along the Kuroshio axis. The rainband suddenly collapsed in the evening

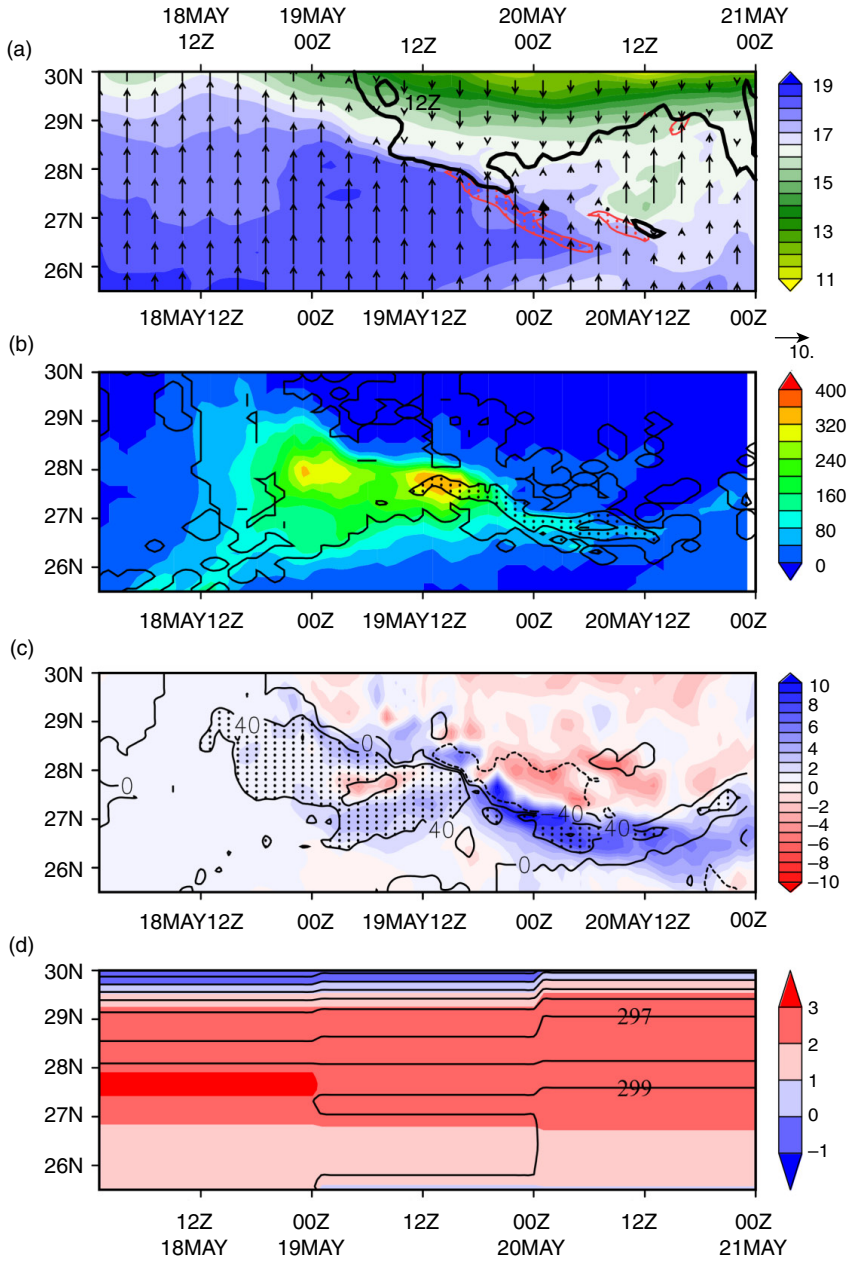

Fig. 4. Time-latitude sections for 126.5°E at 1000 hPa. (a) Specific humidity (g kg^{-1}, shade), meridional wind velocity (m/s, vector), lines of zero meridional velocity (thick black line) and wind convergence greater than 1.0×10^{-4} s^{-1} (red hatch), simulated in the CNTL run. (b) CAPE (J kg^{-1}, shade) and precipitation (mm h^{-1}, contoured for 0 and 1, and hatched for precipitation greater than 1 mm h^{-1}) of the CNTL run. (c) Differences (CNTL minus SMTH) in the column integrated water vapor (kg, shade) and CAPE (J kg^{-1}, contoured for −40, 0 and 40 and hatched for the values greater than 40). (d) SST (K, contour) assigned for the CNTL run, and its difference from its counterpart for the SMTH run (K, shade).

(1300 UTC) of May 20, when CAPE above the Kuroshio was suddenly reduced. This reduction occurred when the extremely moist airmass that had stayed over the warm Kuroshio was replaced with slightly drier air carried by the southerlies blowing toward the Baiu/Meiyu front (Fig. 4a).

The results thus far highlight the potential importance of the narrow band of SST maxima along the Kuroshio in organising the convective rainband, but one may wonder which is more important, the high SST itself or its strong confinement to the current axis. To assess their relative importance, we carried out another experiment

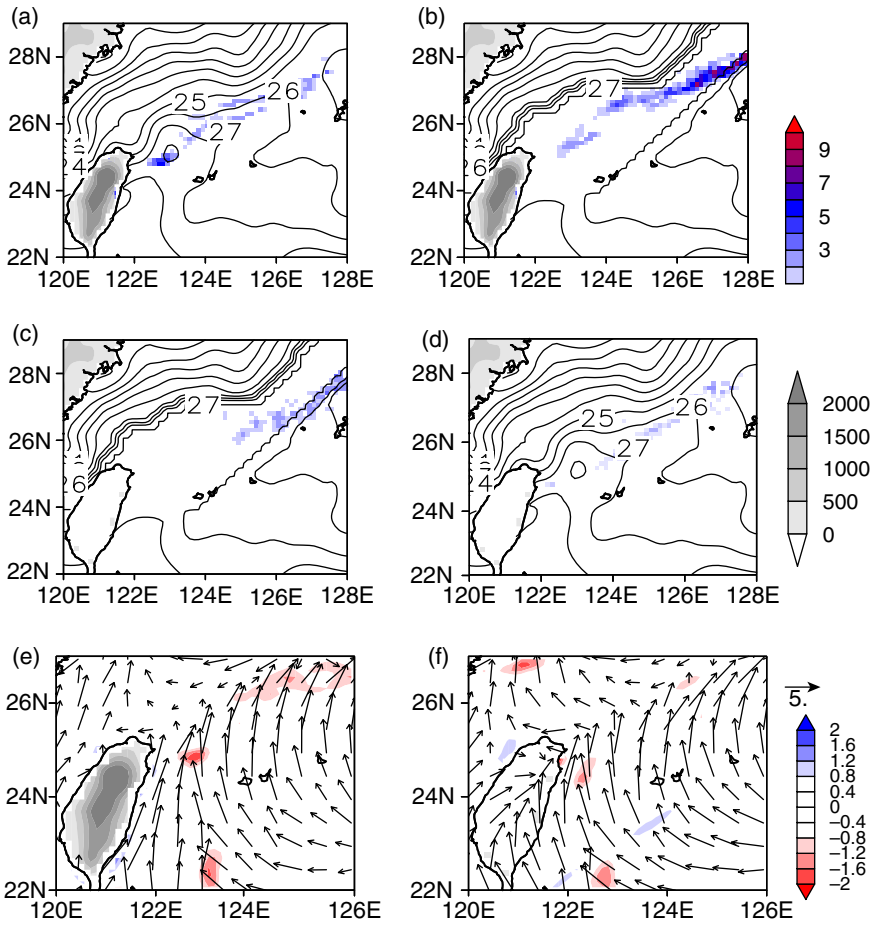

Fig. 5. Results of additional experiments. (a)–(d) Convective precipitation (mm h^{-1}, color shade), land surface elevation (m, gray shade) and SST (°C, contour) of the individual experiments. (a) CNTL run (with realistic topography and observed SST). (b) An experiment where any SST values above 24°C near the Kuroshio have been replaced with a constant value of 27°C. (c) An experiment where the same SST as in (b) has been assigned, but the orography of Taiwan is flattened to no surface elevation. (d) An experiment where the same SST as in the CNTL run with the flattened Taiwan orography as in (c). (e)–(f) 1000-hPa wind velocity (m s^{-1}, vector) and wind divergence over the ocean (10^{-4} s^{-1}, color shade) for the (e) CNTL run and (f) experiment shown in (d). All panels are for 0900 JST (0000 UTC), 20 May 2010.

where any SST values above 24°C associated with the Kuroshio have been replaced with a constant value of 27°C (contoured in Fig. 5b), to remove the well-defined narrow SST maxima along the Kuroshio without lowering SST along its axis unlike in the SMTH run. Corresponding to the flat distribution of high SST, the rainband simulated (colour shade in Fig. 5b) to the east of 124°E becomes broader than its counterpart in the CNTL run (Fig. 5a). To the west, however, the width of the rainband organised to the northeast of Taiwan remains almost unchanged in spite of much more uniform distribution of high SST. Interestingly, the particular rainband is diminished in another experiment (Fig. 5c) where the same SST distribution as in Fig. 5b is assigned but the orography of Taiwan has been eliminated. This particular experiment, however, does not deny the importance of the Kuroshio in the rainband formation. In fact, a companion experiment with *no* Taiwan orography but with the observed SST (Fig. 5d) can reproduce the rainband along the Kuroshio, though slightly weaker than in the CNTL run (Fig. 5a). This is in sharp contrast with Fig. 5c, and the SMTH run (Fig. 2c), in both of which the rainband is almost diminished, especially west of 127.5°E. Therefore, the high SST maxima confined to the Kuroshio axis are an essential factor for organising the rainband, to which Taiwan orography appears to contribute positively. In fact, a comparison between Figs. 5e and 5f reveals that the mountains in Taiwan block the surface southerlies, which appears to weaken the southerlies to the north-east of Taiwan on the cooler flank of the Kuroshio, and thereby enhance the surface convergence (red shade in Fig. 5e, f) over the warm Kuroshio.

4. Summary and discussion

A well-defined convective rainband persisted along the Kuroshio in the East China Sea from 19 May to 20 May 2010, well south of the Baiu/Meiyu front, which suggests the particular importance of local SST maxima along the Kuroshio in the formation of the rainband. This has been verified through a pair of regional atmospheric model integrations, one (CNTL run) with high-resolution SST distribution prescribed and the other (SMTH run) with the corresponding SST field artificially smoothed in space. The CNTL run is successful in reproducing the convective rainband triggered by the poleward intrusion of a convectively unstable humid airmass over high SST along the Kuroshio, while the SMTH run fails to reproduce the rainband. The present study thus presents a striking event where a warm western boundary current *in mid-latitudes* can influence the overlying atmosphere by organising convective clouds, as indicated mainly through statistical analyses by recent studies (Minobe et al., 2008; Tokinaga et al., 2009; Kuwano-Yoshida et al., 2010; Xu et al., 2011; Sasaki et al., 2012). We conjecture that frequent formation of such a convective rainband along the Kuroshio, as identified in the present study, can contribute to climatologically enhanced precipitation in the pre-Baiu period (mid-May through mid-June) near the Okinawa Islands, as shown in Figure 4 of Sampe and Xie (2010). In that period, the region is located well south of the climatological axis of the subtropical jet; therefore, the enhanced precipitation cannot be explained solely by the warm advection of the jet.

One of the most notable features of the rainband is its formation separated from the Baiu/Meiyu front to its north. Recent studies have shown that a multiple-frontal structure is often observed in association with the Baiu/Meiyu front over the East China Sea (Moteki et al., 2004a, 2004b, 2006; Maeda et al., 2008), with emphasis on the confluence of multiple airflows with different characteristics as an important factor for the formation. In fact, as recognised in Fig. 2e, relatively dry air extending northeastward from the west of Taiwan separates an air mass to the north of the Baiu/Meiyu front and another to the south of the Kuroshio axis. Our results for the particular experiment with the flattened terrain over Taiwan (Fig. 5) suggest the potential importance of the orographic effect on enhancing surface convergence over the Kuroshio, thereby setting conditions favourable for organising a rainband well south of the Baiu/Meiyu front. Nevertheless, even in the presence of the Taiwan orography, the structure of the multiple fronts observed with the rainband on 19–20 May 2010 cannot be realised without the high SST along the Kuroshio, as suggested by the SMTH run. Furthermore, even without the Taiwan orography, the rainband structure can be simulated along the Kuroshio as in Fig. 5d. While a more quantitative assessment of the downstream effects of the Taiwan orography on the atmospheric and oceanic conditions is necessary in future study, the present study concludes that high SST along the Kuroshio can be an important factor for yielding multiple frontal structure of the Baiu/Meiyu front over the East China Sea.

We are not quite certain at this stage how frequently a similar convective rainband can form along the Kuroshio over the East China Sea in separation from the Baiu/Meiyu front, which will be another future topic. We have thus far recognised similar events that occurred on 21 June 2010, 23 August 2011, 14 October 2011, 5 March 2012 and 15 May 2012 (not shown). A more comprehensive study is underway on detailed examinations of the individual events with emphasis on their common and different features.

5. Acknowledgements

We thank colleagues in JAMSTEC and Dr. Y. Wang of IPRC, University of Hawaii, for helpful discussions. All the authors are supported in part by the Japanese Ministry of Education, Culture, Sports, Science and Technology (MEXT) through a Grant-in-Aid for Scientific Research in Innovative Areas 2205. HN is also supported by the Japanese Ministry of Environment through the Environment Research and Technology Development Fund A1201.

References

Gregory, D., Morcrette, J. J., Jakob, C., Beljaars, A. C. M. and Stockdale, T. 2000. Revision of convection, radiation and cloud schemes in the ECMWF Integrated Forecasting System. *Q. J. Roy. Meteorol. Soc.* **126**, 1685–1710.

Kosaka, Y., Xie, S.-P. and Nakamura, H. 2011. Dynamics of interannual variability in summer precipitation over East Asia. *J. Clim.* **24**, 5435–5453.

Kuwano-Yoshida, A., Minobe, S. and Xie, S.-P. 2010. Precipitation response to the Gulf Stream in an atmospheric GCM. *J. Clim.* **23**, 3676–3698.

Maeda, S., Tsuboki, K., Moteki, Q., Shinoda, T., Minda, H. and co-authors. 2008. Detailed structure of wind and moisture fields around the Baiu frontal zone over the East China Sea. *SOLA*. **4**, 141–144.

Minobe, S., Kuwano-Yoshida, A., Komori, N., Xie, S.-P. and Small, R. J. 2008. Influence of the Gulf Stream on the troposphere. *Nature*. **452**, 206–209.

Minobe, S., Miyashita, M., Kuwano-Yoshida, A., Tokinaga, H. and Xie, S.-P. 2010. Atmospheric response to the Gulf Stream: Seasonal variations. *J. Clim.* **23**, 3699–3719.

Moteki, Q., Shinoda, T., Shimizu, S., Maeda, S., Minda, H. and co-authors. 2006. Multiple frontal structures in the Baiu frontal zone observed by aircraft on 27 June 2004. *SOLA*. **2**, 132–135.

Moteki, Q., Uyeda, H., Maesaka, T. and Shinoda, T. 2004a. Structure and development of two merged rainbands observed

over the East China Sea during X – BAIU – 99 Part I: Meso-β-scale structure and development processes. *J. Meteorol. Soc. Jpn*. **82**, 19–44.

Moteki, Q., Uyeda, H., Maesaka, T. and Shinoda, T. 2004b. Structure and development of two merged rainbands observed over the East China Sea during X – BAIU – 99 Part II: Meso-α-scale structure and build-up processes of convergence in the Baiu frontal region. *J. Meteorol. Soc. Jpn*. **82**, 45–65.

Ninomiya, K. 1984. Charactaristic of Baiu front as a predominant subtropical front in the summer Northern Hemisphere. *J. Meteorol. Soc. Jpn*. **62**, 880–894.

Nordeng, T. E. 1994. Extended versions of the convective parameterization scheme at ECMWF and their impact on the mean and transient activity of the model in the tropics. *ECMWF. Res. Dept. Tech. Memo*. **206**, 41.

Reynolds, R. W., Smith, T. M., Liu, C., Chelton, D. B., Casey, K. S. and co-authors. 2007. Daily high-resolution-blended analyses for sea surface temperature. *J. Clim*. **20**, 5473–5496.

Sampe, T. and Xie, S. P. 2010. Large-scale dynamics of the Meiyu-Baiu rainband: Environmental forcing by the westerly jet. *J. Clim*. **23**, 113–134.

Sasaki, Y. N., Minobe, S., Asai, T. and Inatsu, M. 2012. Influence of the Kuroshio in the East China Sea on the early summer (Baiu) rain. *J. Clim*. **27**, 6627–6645.

Small, R. J., DeSzoeke, S. P., Xie, S. P., O'Neill, L., Seo, H. and co-authors. 2008. Air-sea interaction over ocean fronts and eddies. *Dyn. Atmos. Oceans*. **45**, 274–319.

Taguchi, B., Nakamura, H., Nonaka, M. and Xie, S. P. 2009. Influences of the Kuroshio/Oyashio extensions on air-sea heat exchanges and storm-track activity as revealed in regional atmospheric model simulations for the 2003/04 cold season. *J. Clim*. **22**, 6536–6560.

Tiedtke, M. 1989. A comprehensive mass flux scheme for cumulus parameterization in large-scale models. *Mon. Wea. Rev*. **117**, 1779–1800.

Tokinaga, H., Tanimoto, Y., Xie, S.-P., Sampe, T., Tomita, H. and co-authors. 2009. Ocean frontal effects on the vertical development of clouds over the Western North Pacific: In situ and satellite observations. *J. Clim*. **22**, 4241–4260.

Wang, Y. 2001. An explicit simulation of tropical cyclones with a triply nested movable mesh primitive equation model: TCM3. Part I: Model description and control experiment. *Mon. Wea. Rev*. **129**, 1370–1394.

Wang, Y., Sen, O. L. and Wang, B. 2003. A highly resolved regional climate model (IPRC-RegCM) and its simulation of the 1998 severe precipitation event over China. Part I: Model description and verification of simulation. *J. Clim*. **16**, 1721–1738.

Wang, Y., Xie, S.-P., Wang, B. and Xu, H. 2005. Large-scale atmospheric forcing by Southeast Pacific boundary layer clouds: A regional model study. *J. Clim*. **18**, 934–951.

Xie, S.-P., Hafner, J., Tanimoto, Y., Liu, W. T., Tokinaga, H. and co-authors. 2002. Bathymetric effect on the winter sea surface temperature and climate of the Yellow and East China Seas. *Geophys. Res. Lett*. **29**, 2228.

Xie, S.-P., Miyama, T., Wang, Y., Xu, H., de Szoeke, S. P., and co-authors. 2007. A regional ocean–atmosphere model for Eastern Pacific climate: Toward reducing tropical biases. *J. Clim*. **20**, 1504–1522.

Xu, H., Xu, M., Xie, S.-P. and Wang, Y. 2011. Deep atmospheric response to the spring Kuroshio over the East China Sea. *J. Clim*. **24**, 4959–4972.